ASTRONOMY & ASTROPHYSICS
SUPPLEMENT SERIES

Astron. Astrophys. Suppl. Ser. **131**, 483–497 (1998)

Integrated spectral study of reddened globular clusters and candidates⋆

E. Bica[1], **J.J. Clariá**[2], **A.E. Piatti**[2], **and C. Bonatto**[1]

[1] Universidade Federal do Rio Grande do Sul, IF, CP 15051, Porto Alegre 91501–970, RS, Brazil
[2] Observatorio Astronómico, Laprida 854, 5000 Córdoba, Argentina

Received January 29; accepted March 23, 1998

Abstract. This paper presents integrated spectra in the range 6700 − 9500 Å for 20 Galactic globular clusters (and candidates) in the bulge and 5 others projected on the Galactic disk ($|l| > 30°$ and $|b| < 5°$). Most of them are considerably reddened and are among those least studied in the literature. We derive reddening and metallicity from flux-calibrated spectra, thus providing independent information of that derived through colour-magnitude studies. For some clusters in the sample, these parameters have been determined for the first time, and for others a considerable revision is given. We indicate the globular clusters which definitely belong to the bulge metal-rich and intermediate metallicity families. Among the objects projected on the disk, we find that the integrated spectral properties of Lyngå 7, BH 176 and Palomar 10 are compatible with those of metal-rich globular clusters. Finally, ESO 93–SC08 is an old open cluster, and UKS 2 is an open cluster with age ≈ 1 Gyr.

Key words: (Galaxy:) globular clusters: general — Galaxy: evolution

1. Introduction

The determination of globular cluster parameters such as reddening and chemical abundances is fundamental to understand their spatial and metallicity distributions, which in turn can be used to study the formation conditions and evolution of the Galaxy (for a recent discussion see van den Bergh 1996). The first step is to determine whether the star cluster is indeed a globular cluster, since the nature of several objects is still unclear. Several compilations provide coordinates, cross-references and available basic data on globular clusters and candidates, e.g. Webbink (1985); Djorgovski & Meylan (1993) and Harris (1996).

Efforts to obtain such parameters have included colour-magnitude diagrams (CMD) and integrated photometry and spectroscopy, see e.g. the compilation of CMDs by Peterson (1986), the integrated photometry by Zinn (1980) and Bica & Pastoriza (1983), the photographic spectroscopy by Zinn & West (1984, hereafter ZW84), and the scanner spectroscopy by Bica & Alloin (1986a). Spectroscopic studies of individual giants in globular clusters provide fundamental abundance determinations, see e.g. the recent results for the metal-poor end of the metallicity scale by Geisler et al. (1995) and Minniti et al. (1996). All these studies have concentrated on the less reddened clusters. The more reddened globular clusters in crowded fields, found in the bulge and low-latitude disk directions, have been studied in a more systematic way only recently. In terms of optical CMDs, several good-quality seeing studies with CCD imaging are providing reliable cluster parameters for difficult objects, e.g. Terzan 5 and HP 1 in the bulge (Ortolani et al. 1996; Ortolani et al. 1997b), Lyngå 7 and Palomar 10 in the disk (Ortolani et al. 1993b; Kaisler et al. 1997). Also in the infrared, where reddening effects are minimised, efforts are being undertaken to explore such clusters by means of CMDs, e.g. Minniti et al. (1995); Frogel et al. (1995) and Guarnieri et al. (1998).

For globular clusters more reddened than $E(B-V) \approx 1.0$, the visible flux becomes too low to provide useful spectra and longer wavelengths should be observed. Bica & Alloin (1987, hereafter BA87) carried out near-infrared CCD integrated spectroscopy of globular clusters in a wide range of metallicity employing the Ca II triplet as metallicity indicator. Armandroff & Zinn (1988, hereafter AZ88) carried out near-infrared CCD spectroscopy for a sample of reddened bulge clusters. They derived metallicities from the Ca II triplet and estimated reddening from an interstellar band at λ8621 Å. However, they have not

Send offprint requests to: E. Bica

⋆ Based on observations made at the Complejo Astronómico El Leoncito (CASLEO), Argentina, and European Southern Observatory (ESO), Chile.

estimated reddening from the continuum distribution, since the spectra were not flux calibrated.

The goal of the present paper is to derive reddening and metallicity for a sample of 20 clusters projected on the bulge ($|l| < 13°$, $|b| < 11°$) and 5 others projected on the disk ($|l| > 30°$ and $|b| < 5°$), by means of flux-calibrated near-infrared spectra. We have 8 clusters in common with AZ88's sample. The objects studied here are part of a systematic spectroscopic survey of globular clusters (and candidates). The first results dealt with 3 candidates which turned out to be emission nebulae (Bica et al. 1995). These objects are: TJ 5 and TJ 23 (Terzan & Ju 1980) which are planetary nebulae, and the one found by Bica (1994) which appears to be a supernova remnant.

This paper is structured as follows: in Sect. 2 we present the observations. In Sect. 3 we derive reddening from the continuum distribution as compared to reddening-free globular cluster template spectra, and metallicity from equivalent widths (W) of the Ca II triplet. Individual objects are discussed in Sects. 4 and 5 respectively for the bulge clusters and the ones projected on the disk. Finally, the conclusions of this work are given in Sect. 6.

2. The observations

The observations were collected with the 2.15 m telescope at the Complejo Astronómico El Leoncito (CASLEO, San Juan, Argentina) in two runs in June 1994 and May 1995. In the first run we employed the Universidade Federal do Rio Grande do Sul (UFRGS) CCD camera attached to the CASLEO Boller & Chivens Spectrograph. The detector is a GEC 6803 chip with 578 × 385 pixels of size 22 μm × 22 μm; one pixel corresponds to 1.″32 on the sky. The slit was oriented E−W except for one exposure of Terzan 1 (Table 1). We used a grating of 300 grooves mm^{-1} producing an average dispersion, in the observed region, of ≈ 240 Å mm^{-1} or 5.4 Å pixel^{-1}. The spectral coverage was ≈ 6400 − 9500 Å. A series of exposures (in general 15 min each) were employed for the objects (Table 1). The long slit, corresponding to 3.′3 on the sky, allowed us to sample regions of background sky. The seeing during the nights was typically ≈ 2.″5. The slit width was 4.″5 resulting in a resolution (FWHM) of ≈ 16 Å as deduced from the comparison lamp lines. Dome and sky flat fields were taken and employed in the reductions. The standard stars CD −32°9927 and LTT 7987 (Stone & Baldwin 1983), and HD 160233 (Gutiérrez-Moreno et al. 1988), were observed for flux calibrations. HD 160233 was also used for the telluric absorption corrections in the near-infrared.

For the second run we used a CCD camera with a Tektronics chip of 1024 × 1024 pixels (of size 24 μm × 24 μm) attached to a REOSC spectrograph. Similar scanning procedures and gratings as in the first run were adopted. The total field along the slit was 4.′7. The range observed corresponds to 5800 − 9200 Å with a dispersion of 3.36 Å pixel^{-1}. The slit width was 4.″2 and the comparison lamp lines provided an average resolution of 17 Å. Two objects (UKS 2 and ESO 93−SC08) have also been observed in the visible range (3500 − 7000 Å) with a dispersion of 140 Å mm^{-1} or 3.46 Å pixel^{-1} leading a resolution of 14 Å. The standard stars were LTT 4364, EG 274 and LTT 7379 as well as HD 160233.

Reductions were carried out with the **IRAF** package following standard procedures at the Instituto de Física, UFRGS (Porto Alegre) and the Córdoba Observatory. The spectra were extracted along the slit according to the cluster size and available flux. For larger objects, we scanned the slit along the N−S direction in order to better sample the cluster stellar population. The resulting spatial coverages are given in Table 1. Wavelength calibrations were carried out with a He-Ne-Ar lamp (He-Ar in the second run) with exposures following that of the object or standard star. The spectra were flux calibrated, and telluric absorption bands were corrected using the hot standard stars following the procedures given by BA87.

Table 1. Logbook of observations

Object	date	Exp.Time (s)	Spatial Window (″ × ″)
Bulge Clusters			
NGC 6256,ESO391–SC6	06/09/94	2×900	4.5×69
TBJ 3,TJ 13	06/12/94	2×900	4.5×22
Terzan 2,HP 3,ESO 454–SC29	06/09/94	3×900	4.5×42
Terzan 4,HP 4,ESO 454–SC7	06/11/94	3×900	4.5×45
HP 1,ESO 455–SC11	06/10/94	2×900	4.5×83
Liller 1	06/10/94	4×900	4.5×35
NGC 6380,Tonantzintla 1, ESO 333–SC14	06/10/94	600+900	4.5×78
Terzan 1,HP 2,ESO 455–SC23	06/10/94	5×900	10×90
Tonantzintla 2,ESO 333–SC16	06/11/94	3×900	10×114
Palomar 6,ESO 520–SC21	06/10/94	3×900	4.5×60
Djorgovski 1	06/12/94	3×900	4.5×34
Terzan 5,ESO 520–SC27	06/10/94	2×900	10×75
Terzan 6,HP 5,ESO 455–SC49	06/10/94	3×900	4.5×65
UKS 1,UKS 1751-241	06/09–10/94	5×900	4.5×39
Terzan 9,ESO 521–SC11	06/09/94	3×900	4.5×39
ESO 456–SC38,Djorgovski 2	06/10/94	3×900	10×50
Terzan 10,ESO 521–SC16	06/09/94	3×900	4.5×65
Terzan 12,ESO 522–SC1	06/12/94	3×900	15×55
Palomar 8,ESO 591–SC12	06/12/94	2×900	4.5×112
NGC 6717,Pal 9,ESO 523–SC14	06/09/94	2×900	10×64
Clusters Projected on the Disk			
BH 176,ESO 224–SC08	06/11/94	3×900	30×70
BH 176,ESO 224–SC08	05/21/95	3×900	30×70
Lyngå 7,BH 184,ESO 178–SC11	06/11/94	3×900	110×93
Lyngå 7,BH 184,ESO 178–SC11	05/21/95	3×900	110×93
Palomar 10	06/12/94	3×900	90×160
Palomar 10	05/21/95	2×900	90×160
UKS 2,UKS 0923-545	06/11/94	3×900	50×80
UKS 2,UKS 0923-545	05/22/95	4×900	50×80
UKS 2,UKS 0923-545 – visible	05/20/95	4×900	50×80
ESO 93–SC08	06/12/94	4×900	10×37
ESO 93–SC08	05/22/95	4×900	10×37
ESO 93–SC08 – visible	05/20/95	4×900	10×37
Control Globular Clusters			
NGC 6528,ESO 456–SC48	06/09/94	600+900	15×63
NGC 6624,ESO 457–SC11	06/10/94	300+600	10×62

Notes: The observations refer to the near-infrared range, except when indicated visible in Col. (1); for Terzan 1, 4 exposures were obtained with an E−W slit at different positions in the N–S direction, and 1 at PA = 58°.

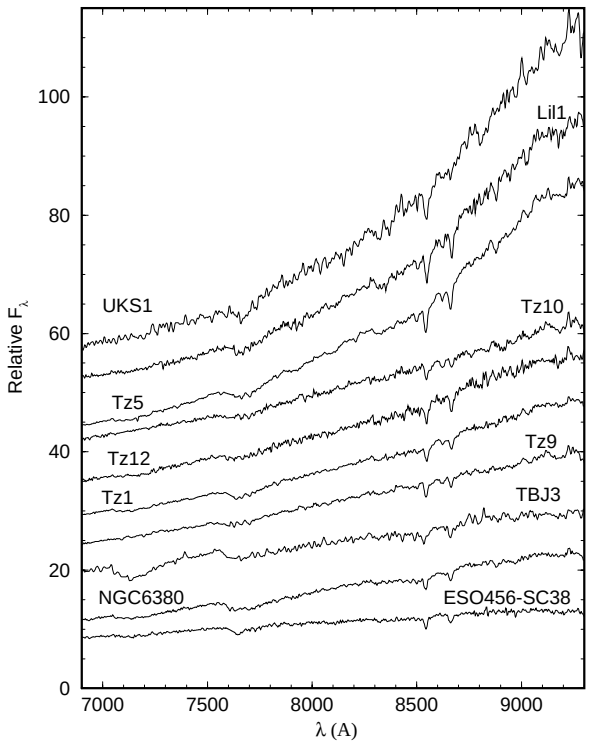

Fig. 1. Observed spectra of bulge objects. Spectra are in F_λ units normalised at $\approx \lambda 7500$ Å. Constants have been added to the spectra, except for the bottom one

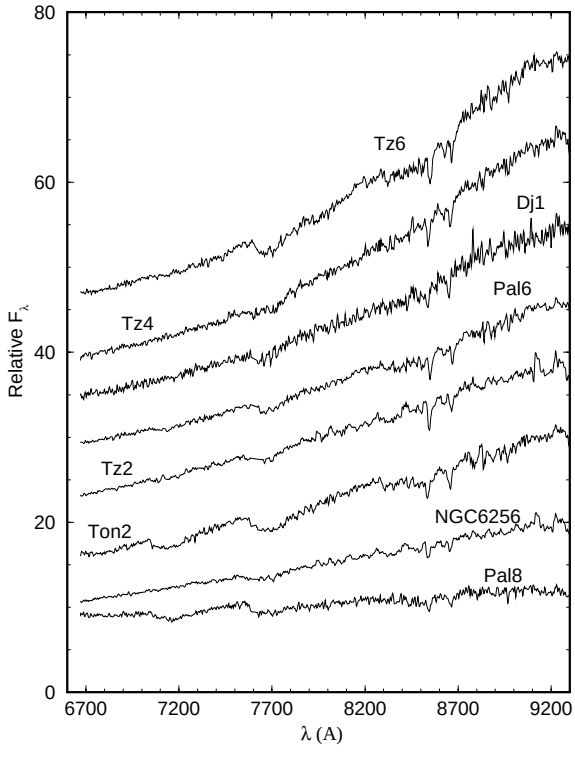

Fig. 2. Same as Fig. 1 for the remaining clusters of the bulge sample

The cluster sample is listed in Table 1. We emphasize that our observations of Terzan 12 refer to the cluster originally designated as such in Terzan (1971) with coordinates $\alpha_{1950} = 18^{\rm h}\ 09^{\rm m}\ 14.0^{\rm s}$ and $\delta_{1950} = -22^\circ\ 45'\ 18''$. We also included in the sample the globular cluster candidate TBJ 3 (Terzan & Bernard 1978).

For comparison purposes we included two well-known bulge clusters NGC 6624 and NGC 6528. The logbook of observations is provided in Table 1, by Cols.: (1) - cluster designations, (2) - date of observation, (3) - number of exposures and duration in seconds, and (4) - slit width (or scanning length) and extraction along the slit (values in arcseconds).

Terzan 1 and Terzan 4 present bright superimposed stars. The different slit positions were checked for the signature of foreground stars by analysing the spectra extracted from individual peaks. In the case of Terzan 1 it was possible to avoid the pixels corresponding to a contaminating foreground late type star which resulted much bluer (thus definitely not as reddened as the cluster) than the remaining cluster extractions, and consequently, it could not be a giant member. In the case of Terzan 4 two foreground stars have been identified and have not been included in the final cluster spectrum.

For HP 1 and NGC 6717 we considered two spatial extractions, a larger one as indicated in Table 1, and a more central extraction for each cluster as discussed respectively in Sects. 4.5 and 4.20.

Figures 1 and 2 show the resulting observed spectra of the bulge sample, and Fig. 3 those projected on the disk. Notice the extremely steep spectra in the upper part of Fig. 1, denoting dramatic dust absorption effects even at these considerably long wavelengths. They correspond to the most reddened globular clusters. The disk objects UKS 2 and ESO 93−SC08 are discussed in Sect. 5.4.

3. Cluster parameters

The Ca II triplet lines ($\lambda\lambda 8498, 8542, 8662$ Å) have been used as metallicity indicators for star clusters in the Galaxy and the LMC, both in integrated spectra (BA87, AZ88) and individual stars (Olszewski et al. 1991).

In order to determine metallicities we measure equivalent widths of the Ca II triplet and compare them to those

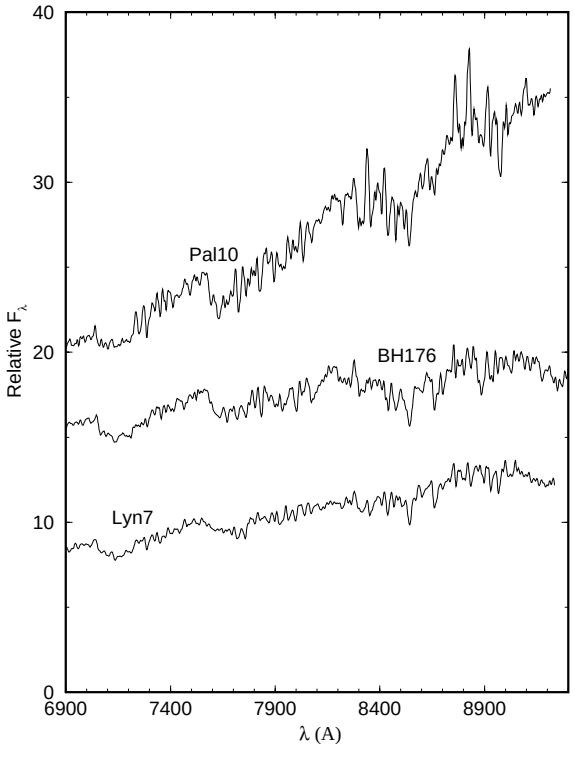

Fig. 3. Same as Fig. 1 for the clusters projected on the disk

of the high Signal/Noise Galactic globular cluster templates G 5 to G 1, ranging from $[Z/Z_\odot] = -2.0$ to nearly-solar metallicity, from Bica (1988). In the case of G 1, the Bica (1988) template has been complemented with the M 31 globular clusters of comparable metallicity G 222 and G 170 (Jablonka et al. 1992) in order to further improve the Signal/Noise ratio. A comparison of an observed cluster spectrum with that of the most similar (reddening-free) template gives the reddening value. The metallicity, in turn, is determined by means of a calibration of the Ws in terms of $[Z/Z_\odot]$.

For the continuum tracing we chose one which minimises TiO contamination, similar to the low one in BA87. CMDs of bulge clusters often present underpopulated giant branches (GB), e.g. Terzan 2 (Ortolani et al. 1997a) and Tonantzintla 2 (Bica et al. 1996). As a consequence, stochastic effects in sampling the cool giants often occur, so that the near-infrared integrated spectrum may present strong (Tonantzintla 2) or weak (Terzan 2) TiO bands (Fig. 6). On the other hand, Ca II arises in all spectral types from F to M (Alloin & Bica 1989), so that it is nearly independent of stochastic effects due to temperature, which makes it a reliable metallicity indicator in the integrated spectrum. Nevertheless, stochastic effects on the giant branch may affect the Ca II triplet significantly, due to the strong gravity dependence (Jones et al. 1984; Alloin & Bica 1989).

Table 2. Equivalent widths (Å)

Object	Ca II$_{\lambda8498}$	Ca II$_{\lambda8542}$	Ca II$_{\lambda8662}$	ΣW
Bulge Clusters				
NGC 6256	1.6	3.3	2.6	7.5
TBJ 3	3.2	5.0	5.1	13.3
Terzan 2	1.6	4.3	3.6	9.5
Terzan 4	0.9	3.4	3.3	7.6
HP 1 (total)	1.8	3.9	3.0	8.7
HP 1 (core)	1.1	3.2	2.7	7.0
Liller 1	2.6	5.6	5.4	13.6
NGC 6380	2.2	4.1	3.1	9.4
Terzan 1	1.9	4.3	4.0	10.2
Tonantzintla 2	2.8	4.8	4.6	12.2
Palomar 6	2.6	4.3	4.3	11.2
Djorgovski 1	2.2	3.1	3.2	8.5
Terzan 5	2.9	5.5	5.1	13.5
Terzan 6	2.8	4.8	4.5	12.1
UKS 1	1.7	5.0	4.4	11.1
Terzan 9	1.4	3.5	2.6	7.5
ESO 456−SC38	1.3	3.8	4.1	9.2
Terzan 10	0.8	3.2	2.8	6.8
Terzan 12	2.2	4.8	4.5	11.5
Palomar 8	2.6	4.0	3.8	10.4
NGC 6717 (total)	1.7	3.4	3.0	8.1
NGC 6717 (core)	2.0	3.9	3.3	9.2
NGC 6717 (decontam.)	1.3	2.9	3.0	7.2
Clusters Projected on the Disk				
BH 176	3.7	6.5	5.6	15.4
Lyngå 7	1.9	4.4	3.0	9.3
Palomar 10	5.0	7.0	5.7	17.7
UKS 2	1.3	4.5	4.8	10.6
ESO 93−SC08	1.3	4.0	3.7	9.0
Control Clusters				
NGC 6528	3.0	5.5	4.2	12.7
NGC 6624	1.3	3.5	3.0	7.8
47 Tuc	1.5	3.4	2.7	7.6
Globular Cluster Templates				
G 1	3.1	5.0	4.3	12.4
G 2	1.9	3.7	3.4	9.0
G 3	1.5	2.9	3.1	7.5
G 4	1.1	2.3	2.8	6.2
G 5	1.1	1.8	2.2	5.1

The adopted continuum points are at $\lambda \approx 8372$ Å and $\lambda \approx 8838$ Å, with a pivot point at $\lambda \approx 8584$ Å, if necessary. For the three Ca II lines the windows are from BA87: 8476 − 8520 Å, 8520 − 8564 Å and 8640 − 8700 Å. The resulting Ws are listed in Cols. 2−4 of Table 2, together with their sum (Col. 5). Typical errors were estimated from uncertainties in the continuum level and resulted in the range 5 − 10%. For comparison and calibration purposes, Ca II triplet Ws were also measured in the same way for the templates G 1 to G 5 (Table 2).

3.1. Reddening

Ideally, the best spectroscopic method to determine reddening for star clusters is to have available reddening-free template spectra of similar properties, and to use a wavelength baseline as wide as possible, as in the recent study of globular clusters in NGC 5128 by Jablonka et al. (1996). Although the present wavelength range is limited to the near-infrared, it can be used to constrain the reddening values.

Guided by the sum of Ws of the Ca II triplet (ΣW) we identify among the templates that resembling most the cluster spectrum. Subsequently, a Seaton (1979) law was applied to derive $E(B-V)$. This method is illustrated in Fig. 4 for Terzan 5 and Terzan 9 with corresponding templates G 1 and G 3, respectively. The templates and derived $E(B-V)$ for each cluster are given in Table 3. We present in Figs. 5 and 6 reddening-corrected spectra for the bulge sample. Notice that in the very reddened clusters UKS 1 and Liller 1 (respectively $E(B-V)=3.1$ and 2.8) a strong absorption feature occurs at $\lambda \approx 7550-7850$ Å. We emphasise that the present spectra are corrected for the telluric A band (Sect. 2). A similar strong feature was observed in the extremely reddened ($E(B-V)=4.4$) open cluster Westerlund 1 (Piatti et al. 1998). This feature appears to be a diffuse interstellar band (Sanner et al. 1978) and the present results suggest that the band is detectable in spectra of globular clusters more reddened than $E(B-V)=1.5$, and becomes prominent for $E(B-V)\geq 2$ (see Figs. 4, 5 and 6). The diffuse interstellar band occurs in the same spectral region as TiO stellar bands and they are certainly blended in several spectra. However, the TiO absorption at $\lambda 7100-7300$ Å might be used to infer the relative proportions of the absorptions in the region $\lambda \approx 7550-7850$ Å.

The strong-lined clusters projected on the disk result of $\approx$ solar metallicity (Sect. 3.2), and their reddening-corrected spectra are shown in Fig. 7. The templates used in the matchings were the metal-rich globular cluster templates G 1 and G 2 (Table 3). Similar to CMD studies, which so far have not been able to establish the real nature of these objects as globular clusters or very old open clusters, owing to crowding and reddening effects, the present spectroscopic results are not conclusive, but the spectra are consistent with those of very old clusters.

The bulge clusters HP 1 and NGC 6717 with 2 spatial extractions are shown in Figs. 8 and 9 respectively (see Sects. 4.5 and 4.20).

3.2. Metallicity

The correspondence between the metallicity scales [Fe/H] and $[Z/Z_\odot]$ is not a trivial issue, rather it is a fundamental matter of debate (for a recent discussion of metal-rich globular clusters see Bruzual et al. 1997). For the sake of simplicity, we adopt in what follows the original scales given by each author. To calibrate our data we employed a $[Z/Z_\odot]$ scale.

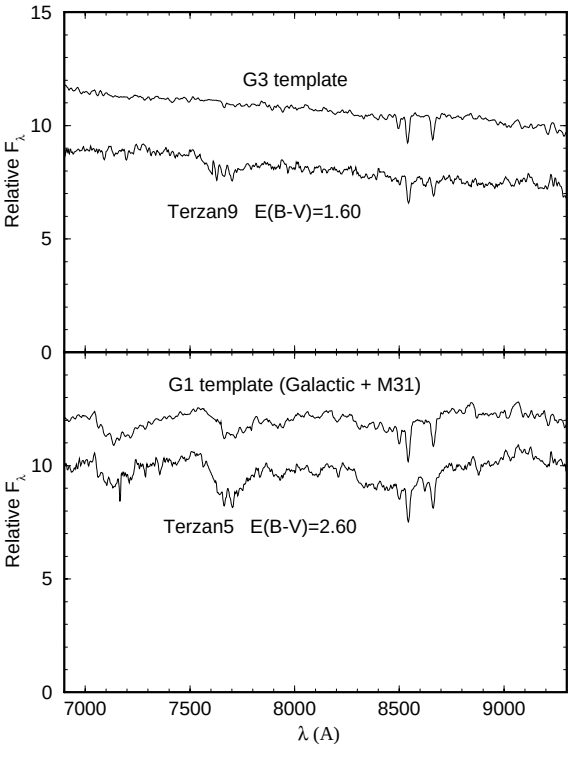

Fig. 4. Top panel: comparison of the reddening-corrected Terzan 9 spectrum to the $[Z/Z_\odot]\approx -1.0$ G 3 template. Bottom panel: comparison of the reddening-corrected Terzan 5 spectrum to the $[Z/Z_\odot]\approx 0.0$ G 1 template, including Galactic and M 31 globular clusters

We calibrated ΣW as a function of metallicity adopting $[Z/Z_\odot]=0.0,-0.5,-1.0,-1.5$ and -2.0 respectively for the templates G 1, G 2, G 3, G 4 and G 5. This calibration is based on individual $[Z/Z_\odot]$ of clusters in each template and a grid of Ws as a function of metallicity (Bica & Alloin 1986a,b; BA87; Bica 1988). The metallicity scale is similar to that of ZW84 and the ones in Jablonka (1992) and Jablonka et al. (1996).

The control clusters NGC 6528 and NGC 6624 (Table 1), as well as 47 Tucanae, have been used in the calibration, adopting metallicity values from ZW84. The near-infrared spectrum of 47 Tuc is from Bica et al. (1992). The resulting calibration curve is shown in Fig. 10, and the derived $[Z/Z_\odot]$ values for the sample clusters are given in Col. 4 of Table 3.

The abundance calibration of the metal-rich end is a fundamental problem in stellar populations. The calibration problem has been recently addressed by means of

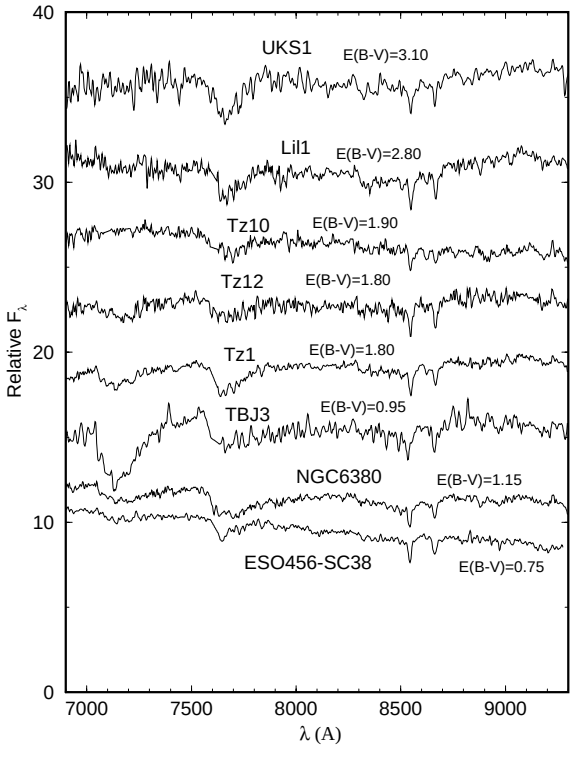

Fig. 5. Reddening-corrected spectra for bulge clusters

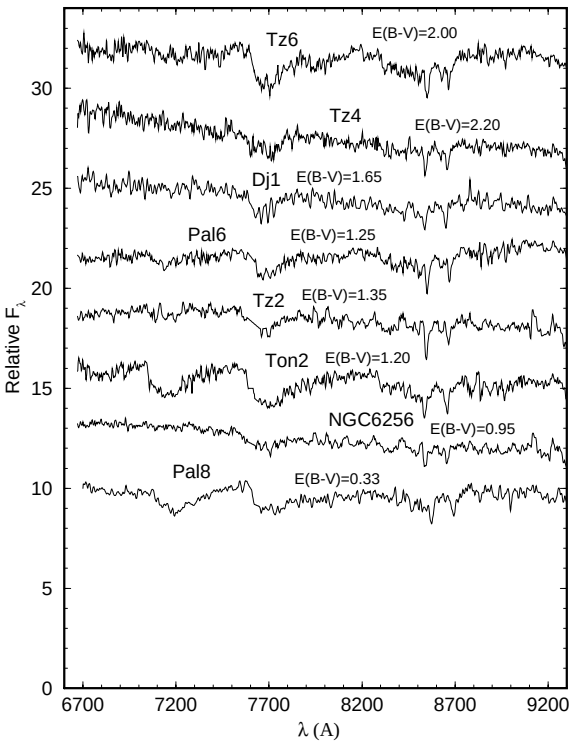

Fig. 6. Same as Fig. 5 for the remaining bulge clusters in the sample

high dispersion spectra of individual stars by Barbuy et al. (1992, 1997), deep colour magnitude diagrams by Ortolani et al. (1995), and integrated spectra (Santos et al. 1995), in the study of the nearly-solar metallicity key globular clusters NGC 6553 and NGC 6528 (which are part of the G 1 template). The iron abundance [Fe/H] in such clusters appears to be somewhat under solar ([Fe/H] $\approx -0.2/-0.3$), whereas [α-elements/Fe] are enhanced, resulting in an overall metallicity $[Z/Z_\odot] \approx 0.0$, as herein adopted for the G 1 template.

Typical errors in $[Z/Z_\odot]$ implied by uncertainties in the Ws are $\approx \pm 0.15$ dex. However, owing to the fact that these bulge regions are very crowded, contamination effects by field stars on the cluster and background regions, uncertainties may be larger for some clusters. The present values should be taken as indicative, and for definitive results for each cluster complementary information from deep CMDs and spectroscopy of individual member giants would be necessary.

4. Bulge objects

Since care is necessary to interpret reddened integrated spectra in such crowded regions, we discuss in this section individual clusters comparing the present results with previous ones from the literature, especially with those from CMDs, when available.

Different techniques have been most frequently used to study such clusters: Malkan (1982, hereafter M82) derived reddening from integrated infrared photometry; ZW84 and Zinn (1985, hereafter Z85) based on the same data, estimated metallicities [Fe/H]. By means of near-infrared integrated spectra AZ88 derived [Fe/H] from the Ca II triplet, and reddening from the interstellar band at 8621 Å. Origlia et al. (1997) derived [Fe/H] by means of infrared integrated spectra using a calibration of the 1.62 μm feature (mostly CO). Minniti (1995) employed (J, K) photometry and visible spectroscopy of giants in the clusters. Finally, information from (V, I, z) and (J, K) CMDs are available for many clusters as discussed below in conjunction with the present spectroscopic results. In particular, (V, I) CMDs are a very sensitive metallicity discriminator among metal-rich clusters, owing to curvature effects on the GB by blanketing effects (Ortolani et al. 1991).

Taking into account the growing body of evidence that the HB morphology is related to the cluster structure (Buonanno et al. 1997 and references therein), we also

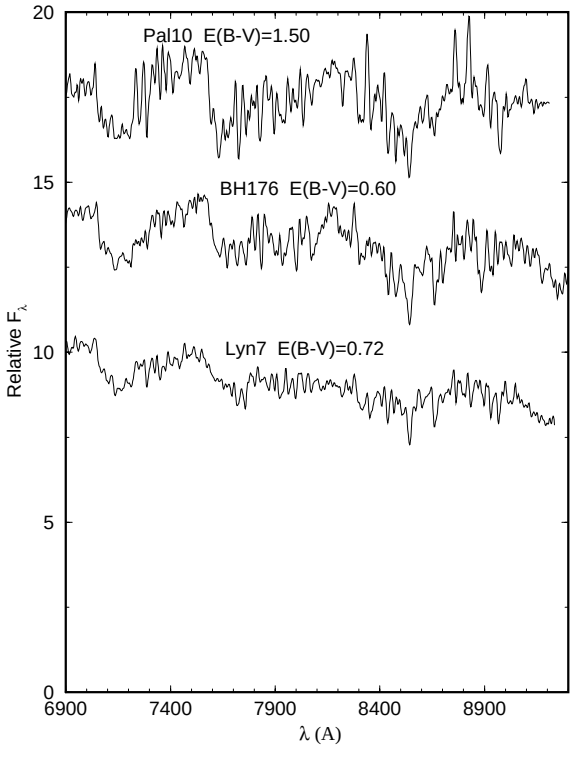

Fig. 7. Same as Fig. 5 for clusters projected on the disk

indicate for each cluster the HB characteristics from CMDs, and structural analysis results, whenever available, in view of a future test of these ideas for bulge clusters, as improved CMDs will become available.

4.1. NGC 6256

In an early photographic study, Alcaino (1983) obtained a B,V CMD with detection limit at the HB level, and estimated $E(B-V) = 0.80$ and a metallicity comparable to that of 47 Tuc. However, a deeper CCD photometry (Ortolani et al. 1998) shows a blue-extended HB similar to that of the intermediate metallicity cluster NGC 6522 (Barbuy et al. 1994).

The derived spectroscopic $[Z/Z_\odot] = -1.01$ (Table 3), indicates a lower metallicity than that of 47 Tuc. This value might still be an upper limit, owing to possible metal-rich field star contamination. We remind that the cluster NGC 6256 is in a post-core collapse phase (Trager et al. 1995, hereafter TKD95). NGC 6256 appears to belong to an intermediate metallicity bulge family (IMBF) like NGC 6522 itself and NGC 6540 (Bica et al. 1994), which are characterised by blue-extended HBs and a post-core collapse structure.

Table 3. Derived parameters

Object	Template	$E(B-V)$	$[Z/Z_\odot]$
Bulge Clusters			
NGC 6256	G 3	0.95	−1.01
TBJ 3	G 1	0.95	+0.06
Terzan 2	G 2	1.35	−0.26
Terzan 4	G 3	2.20	−0.61†
HP 1 (total)	G 2	1.10	−0.37†
HP 1 (core)	G 3	1.00	−1.09
Liller 1	G 1	2.80	+0.08
NGC 6380	G 2	1.15	−0.27
Terzan 1	G 1	1.80	−0.18
Tonantzintla 2	G 1	1.20	−0.01
Palomar 6	G 1	1.25	−0.09
Djorgovski 1	G 2	1.65	−0.40
Terzan 5	G 1	2.60	+0.07
Terzan 6	G 1	2.00	−0.02
UKS 1	G 1	3.10	−0.10
Terzan 9	G 3	1.60	−1.01
ESO 456−SC38	G 2	0.75	−0.30
Terzan 10	G 4/G 3	1.90	−1.35
Terzan 12	G 1	1.80	−0.06
Palomar 8	G 1	0.33	−0.16
NGC 6717 (total)	G 3	0.21	−0.47†
NGC 6717 (core)	G 2/G 3	0.10	−0.30†
NGC 6717 (decontaminated)	G 3	–	−1.05
Clusters Projected on the Disk			
BH 176	G 1	0.60	$> +0.1$
Lyngå 7	G 2	0.72	−0.28
Palomar 10	G 1	1.50	$> +0.1$
UKS 2	I 1	0.20	−0.15
ESO 93−SC08	I 2/G 2	0.35	−0.34

Notes: $[Z/Z_\odot]$ obtained from the calibration of ΣW of the Ca II triplet (Fig. 10). † - important contamination by metal-rich bulge stars.

4.2. TBJ 3 = TJ 13

This object at $\alpha(1950) = 17^{\rm h}\ 15^{\rm m}\ 06^{\rm s}$ and $\delta(1950) = -27^\circ\ 51'$, is the only remaining globular cluster candidate in the lists of Terzan & Bernard (1978) and Terzan & Ju (1980). Djorgovski et al. (1990) found that TBJ 1 = TJ 17 with radial velocity $V_R = 6270\,{\rm km\,s^{-1}}$ and TJ 15 with $V_R = 8619\,{\rm km\,s^{-1}}$ are galaxies. They also reported images of these objects together with TBJ 2 = TJ 16 indicating their galaxy nature. Finally, TJ 5 and TJ 23 are planetary nebulae (Bica et al. 1995).

The integrated spectrum (Fig. 1) presents no evidence of a redshifted component, indicating that the dominant light source is not a background galaxy. Terzan & Bernard (1978) presented an R plate of TBJ 3 and described the object as circular and diffuse with a diameter of $\approx 10''$. An R CCD image taken in May 1994 with the Danish telescope at ESO, La Silla, showed that the central clump is partially resolved into stars, and a faint halo of stars might be present (Ortolani, private communication).

The spectral properties are compatible with those of a metal-rich globular cluster like NGC 6528 (Table 2 and Fig. 5). The derived reddening ($E(B-V) = 0.95$) is not as large as those of the very reddened bulge clusters (Table 3). As discussed by e.g. Aguilar (1993), there are several dynamical processes which might lead to the destruction of globular clusters, such as mass loss, tidal shocks, dynamical friction, and disruption of clusters venturing the central 2 kpc. In this respect the appearance and spectrum of TBJ 3, together with the moderate reddening for this faint object, places TBJ 3 as a candidate for a low luminosity post-core collapse fossil of a globular cluster. We note, however, that some bulge stars might be dominating the observed spectrum, and the derived reddening would be, in this case, a lower limit so that TBJ 3 might be a more distant and luminous object. Deep CMDs would be necessary to establish the nature of this interesting object.

4.3. Terzan 2

The different techniques provided quite similar reddening and metallicity values. The infrared integrated photometry indicated $E(B-V) = 1.3$ and [Fe/H] $= -0.47$ (M82/ZW84/Z85); AZ88 derived $E(B-V) = 1.54$ and [Fe/H] $= -0.25$; Kuchinski et al. (1995) employed K, $(J-K)$ CMDs and estimated [Fe/H] $= -0.25$; Ortolani et al. (1997a) employed V, $(V-I)$ CMD and derived $E(B-V) = 1.54$ and [Fe/H] $= -0.55$.

The reddening and metallicity derived in Table 3 are consistent with the previous results. This cluster belongs to the metal-rich bulge family (MRBF) and is in a post-core collapse phase (TKD95).

4.4. Terzan 4

From integrated infrared photometry, M82/ZW84/Z85 obtained $E(B-V) = 1.5$ and [Fe/H] $= -0.21$; AZ88 found $E(B-V) = 1.52$ and [Fe/H] $= -0.94$ from near-infrared spectroscopy; Ortolani et al. (1997) used a deep ESO NTT V, $(V-I)$ CMD (under exceptional seeing conditions $0\farcs35 - 0\farcs55$) and detected a blue HB and a general morphology which might place this cluster as metal-poor as [Fe/H] $= -2.0$. They derived a high reddening $E(B-V) = 2.35$, which suggests that contamination by foreground field stars affected previous determinations.

In the present study we have eliminated pixel rows to avoid two obvious foreground (less reddened) bright stars (Sect. 2). Indeed, the resulting $E(B-V)$ for the cluster (Table 3), is close to that derived from the CMD. However, the metallicity (Table 3) is high as compared to that from the CMD, suggesting that metal-rich bulge stars reddened as much as the cluster affect the present spectrum. We conclude that Terzan 4 is not a member of the MRBF.

4.5. HP 1

The near-infrared spectroscopy provided $E(B-V) = 1.44$ and [Fe/H] $= -0.56$ (AZ88). From individualgiants, Minniti (1995) obtained $E(B-V) = 1.68$ and [Fe/H] $= -0.30$, and Minniti et al. (1995) favoured $E(B-V) = 1.25$ and [Fe/H] $= -0.5$ from a K, $(J-K)$ CMD. On the other hand, the deep V, $(V-I)$ CMDs in Ortolani et al. (1997b) revealed that HP 1 has a blue extended HB and a general morphology of a globular cluster with [Fe/H] ≈ -1.5; they obtained a reddening $E(B-V) = 1.19$.

In the present study we analyse two spatial extractions of HP 1: that of Table 1 corresponding to $83''$ along the slit, and a core extraction of $10''$ along the slit. The observed and reddening-corrected spectra are shown in Fig. 8, while the equivalent width values are given in Table 2. The core spectrum provides a low metallicity $[Z/Z_\odot] = -1.09$ (Table 3), while the total spectrum is considerably contaminated by metal-rich stars ($[Z/Z_\odot] = -0.37$). This radial change explains why high values of metallicity have been obtained in previous studies. The present metallicity of the core is possibly still an upper limit, but taking into account the CMD results of Ortolani et al. (1997b), we confirm that HP 1 belongs to the IMBF, likewise NGC 6256 (Sect. 4.1) with post-core collapse (TKD95). The present reddening value is consistent with the previous lower values.

Interestingly, metal-rich stars at the same distance as the cluster are seen in the CMD (Ortolani et al. 1997b). They define tighter sequences than would be expected from depth and differential reddening effects for the bulge field, which led Bica et al. (1997) to consider the possibility of capture of such stars by globular clusters in dense bulge fields. The mechanism appears to be efficient enough to change significantly the stellar population content of a globular cluster over a Hubble time. The metallicity contrast produced by this effect would be more pronounced in metal-poor clusters like HP 1. It is expected to operate as well in metal-rich bulge family clusters, although in this case the effect would be difficult to detect.

Another interesting mechanism which might create composite CMDs is that of mergers (Catelan 1997). This effect would require that mergers have previously occurred in dwarf galaxies like Sagittarius, because the velocity dispersion of globular clusters in the bulge is exceedingly high. Consequently, one would not expect the very metal-rich globular clusters to take part in a merger event.

4.6. Liller 1

From integrated infrared photometry, M82/ZW84/Z85 obtained $E(B-V) = 2.9$ and [Fe/H] $= -0.21$; AZ88 derived $E(B-V) = 2.71$ and [Fe/H] $= +0.20$; Origlia et al. (1997) found [Fe/H] $= -0.29$; Frogel et al. (1995) employed K, $(J-K)$ CMD and derived [Fe/H] $= +0.25$.

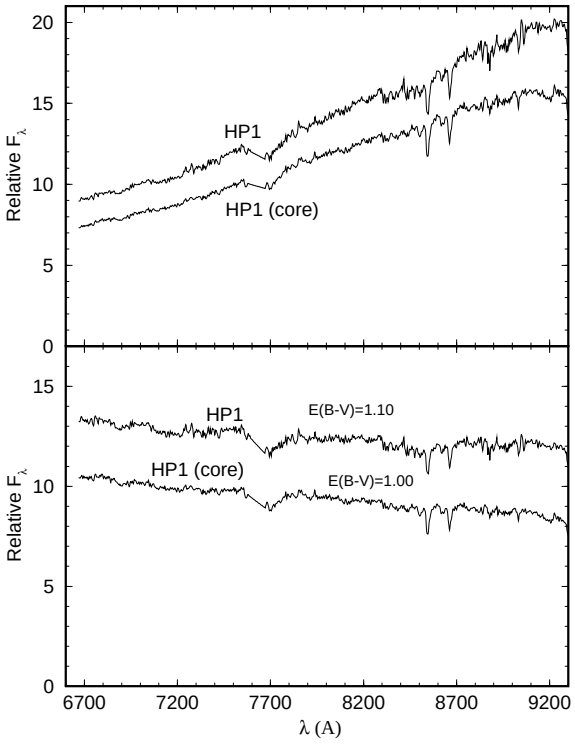

Fig. 8. HP 1: different extractions. Top panel, observed spectra; bottom panel, reddening-corrected

Finally, Ortolani et al. (1996) from an I, $(I-z)$ CMD found $E(B-V)=3.05$ and [Fe/H] comparable to that of the inner bulge stellar population.

The values obtained in Table 3 for reddening and metallicity confirm the previous results. The cluster belongs to the MRBF and is possibly among the most metal-rich ones. Deeper studies are necessary for a definitive diagnosis. The cluster is very concentrated and possibly is in a post-core collapse phase (Trager et al. 1993, hereafter TDK93).

4.7. NGC 6380

The integrated infrared photometry (M82/ZW84/Z85) provided $E(B-V)=1.4$ and [Fe/H] $=-1.0$. On the other hand, Ortolani et al. (1998) using V, $(V-I)$ CMDs found GB and HB morphologies of a metal-rich globular cluster, deriving [Fe/H] ≈ -0.5, and a lower reddening value $E(B-V)=1.07$.

The present results (Table 3) are consistent with the latter study, placing NGC 6380 in the MRBF. TDK95 pointed out NGC 6380 as a possible post-core collapse cluster, however, Ortolani et al. (1998) did not find any evidence of this effect using ESO NTT images with $1''$ seeing.

4.8. Terzan 1

The integrated infrared photometry provided $E(B-V)=1.5$ and [Fe/H] $=+0.24$ (M82/ZW84/Z85) while the integrated near-infrared spectroscopy by AZ88 indicated a similar reddening $E(B-V)=1.49$ and a lower metallicity [Fe/H] $=-0.71$, albeit still placing the cluster in the metal-rich family. Ortolani et al. (1993a) using (V, I, z) CMDs found evidence of a high metallicity for this cluster, from the strong curvature effects on the GB, and also derived $E(B-V)=1.67$. Bica et al. (1993) pointed out the occurrence of two relatively bright disk blue main sequence stars close to the cluster core which might explain a dilution of the Ca II triplet, and consequently, the lower metallicity value derived by AZ88. From integrated infrared spectroscopy, Origlia et al. (1997) derived a high metallicity, [Fe/H] $=+0.03$.

The present integrated spectrum shown in Fig. 1 samples a large area, $10''\times 90''$ (Table 1) and should represent as much as possible the cluster global properties. As explained in Sect. 2, the pixels corresponding to a bright foreground (much less reddened than the cluster) late-type giant have been excluded. The derived reddening is $E(B-V)=1.80$ (Table 3), and the resulting reddening-corrected spectrum (Fig. 5) clearly shows absorption features characteristic of a very metal-rich cluster. The derived metallicity $[Z/Z_\odot]=-0.18$ places Terzan 1 nearly at the solar value. We cannot rule out some contamination either by blue disk stars which would dilute the Ca II triplet, or bulge/disk red stars which would enhance the metallicity, with a reddening comparable to that of the cluster. We conclude that Terzan 1 is a member of the MRBF, probably one of the most metal-rich clusters with post-core collapse (TKD95).

4.9. Tonantzintla 2

The (V, I) CMDs in Bica et al. (1996) showed GB and HB morphologies of a metal-rich globular cluster, and they derived $E(B-V)=1.26$ and [Fe/H] $=-0.60$.

The spectroscopic reddening and metallicity (Table 3) confirm the latter results, placing Tonantzintla 2 as a new member of the MRBF. The cluster is not in a post-core collapse phase (TDK95).

4.10. Palomar 6

The integrated infrared photometry (M82/ZW84/Z85) provided $E(B-V)=1.4$ and [Fe/H] $=-0.74$; Minniti et al. (1995) derived $E(B-V)=1.63$ and [Fe/H] $=+0.20$; Minniti et al. (1995) from K, $(J-K)$ CMD

favoured $E(B-V) = 1.25$ and [Fe/H] $= +0.2$; finally, Ortolani et al. (1995a) using (V, I) CMDs found GB and HB morphologies of a metal-rich globular cluster, deriving $E(B-V) = 1.33$ and [Fe/H] $= -0.4$. Although there is some dispersion in the metallicity values, all studies agree that Palomar 6 is a MRBF.

The present metallicity value $[Z/Z_{\odot}] = -0.09$ (Table 3) is consistent with the average of the previous results, and favours the lower reddening values. Palomar 6 is not in a post-core collapse phase (TDK95).

4.11. Djorgovski 1

Ortolani et al. (1995a) using (V, I) CMDs found GB and HB morphologies of a metal-rich globular cluster, deriving $E(B-V) = 1.71$ and [Fe/H] $= -0.4$.

The present determinations (Table 3) agree well. This cluster belongs to the MRBF. The cluster structure is somewhat loose with a concentration parameter $c = 1.50$, and there is no evidence of post-core collapse (TDK93, see also the image in Ortolani et al. 1995a).

4.12. Terzan 5

The integrated infrared photometry (M82/ZW84/Z85) provided $E(B-V) = 2.1$ and [Fe/H] $= +0.24$; AZ88 derived $E(B-V) = 1.65$ and [Fe/H] $= -0.28$; Liu et al. (1994) employed a K', $(J-K')$ CMD, and derived $E(B-V) = 1.6$ and [Fe/H] $= -0.3$; Origlia et al. (1997) derived [Fe/H] $= -0.64$; and Ortolani et al. (1996) from (V, I) CMDs found GB and HB morphologies of a very metal-rich globular cluster, obtaining [Fe/H] $= 0.0$ and $E(B-V) = 2.49$.

The different studies present a considerable range of reddening values, and the present result ($E(B-V) = 2.60$) is consistent with the higher estimates. A range in metallicity is also present in the literature, but all agree in the sense that the cluster is metal-rich and the present value ($[Z/Z_{\odot}] = +0.07$) is consistent with the higher estimates. The cluster is MRBF and is not in a post-core collapse phase (TDK95).

4.13. Terzan 6

The near-infrared spectroscopy indicated $E(B-V) = 2.93$ and [Fe/H] $= -0.61$ (AZ88); Barbuy et al. (1997) using (V, I, z) CMDs found GB and HB morphologies of a metal-rich globular cluster, deriving $E(B-V) = 2.24$ and a metallicity intermediate between those of 47 Tuc and NGC 6528/6553.

The reddening in Table 3 is consistent with that derived from (V, I) CMDs; the reddening in AZ88 is exceedingly high. The metallicity found in all studies places the cluster in the MRBF. The cluster is in a post-core collapse phase (TKD95).

4.14. UKS 1

The integrated infrared photometry (M82/ZW84/Z85) provided $E(B-V) = 3.1$ and [Fe/H] $= -1.18$; Liu et al. (1994) estimated $E(B-V) = 2.8$ and [Fe/H] $= -1.2$ from infrared CMDs; Minniti et al. (1995) showed a K, $(J-K)$ CMD detecting the GB; Ortolani et al. (1997c) using I, $(I-z)$ CMDs also detected the GB consistent with a very reddened globular cluster with $E(B-V) = 3.1$.

The present value (Table 3) confirms the high reddening. However, the near-infrared reddening-corrected spectrum (Fig. 4) and absorption features (Table 2) are those of a metal-rich globular cluster. If metal-rich bulge stars contribute to the integrated light of UKS 1, they must be nearly at the cluster distance, since there is no change in $E(B-V)$ as deduced from the CMDs. Deeper studies are necessary for a definitive diagnosis of this cluster. The cluster is rather concentrated and may be in a post-core collapse phase (TDK93, see also the CCD image in Ortolani et al. 1997c).

4.15. Terzan 9

The integrated infrared photometry (M82/ZW84/Z85) provided $E(B-V) = 1.7$ and [Fe/H] $= -0.38$; AZ88 derived lower values for reddening and metallicity ($E(B-V) = 1.25$ and [Fe/H] $= -0.99$); Liu et al. (1994) obtained $E(B-V) = 1.8$ and [Fe/H] $= -1.0$.

The present reddening ($E(B-V) = 1.60$) is consistent with the highest values found, and the metallicity ($[Z/Z_{\odot}] = -1.01$) with the lower estimates. The cluster probably does not belong to the MRBF, and deep CMDs, including the HB morphology, are necessary for a more conclusive result. The cluster is in a post-core collapse phase (TKD95).

4.16. ESO 456−SC38

By means of V, $(V-I)$ CMDs, Ortolani et al. (1997c) found evidence of a metal-rich GB. They derived [Fe/H] $= -0.5$ and $E(B-V) = 0.89$.

The reddening and metallicity in Table 3 are consistent with the (V, I) CMD results, placing the cluster in the MRBF. The cluster structure is rather loose with a concentration parameter $c = 1.50$, and there is no evidence of post-core collapse (TDK93). See also the image in Ortolani et al. (1997c), where some central bright sources appear to be stars.

4.17. Terzan 10

Liu et al. (1994) estimated $E(B-V) = 2.6$ and [Fe/H] $= -0.7$ from an infrared CMD. Ortolani et al. (1997c) using

V, $(V-I)$ CMDs detected the GB (and possibly some evidence of a blue HB) and derived $E(B-V)=2.40$.

The integrated spectrum indicates an intermediate metallicity ($[Z/Z_{\odot}] = -1.35$ and $E(B-V) = 1.90$, Table 3). The reddening value is somewhat lower than those from the CMD studies, which might suggest some contamination by foreground stars (bulge or disk). Taking together the evidence of a blue HB and the present metallicity value, Terzan 10 probably belongs to the IMBF, unless contamination by field stars affects the estimate. However, differently of the other IMBF clusters discussed in the present paper, the CCD image of Terzan 10 in Ortolani et al. (1997c) shows no evidence of post-core collapse, where the bright sources superimposed appear to be bright stars. Deeper studies are necessary for a definitive diagnosis of this cluster.

4.18. Terzan 12

Ortolani et al. (1998) using V, $(V-I)$ CMDs found GB and HB morphologies of a metal-rich globular cluster, deriving $E(B-V)=2.06$ and [Fe/H] ≈ -0.5.

The present values (Table 3) basically confirm these results. The cluster is a new member of the MRBF and is not in a post-core collapse phase (TDK95, therein referred to as Terzan 11). The image in Ortolani et al. (1998) supports the latter result.

4.19. Palomar 8

A visible integrated spectrum indicated [Fe/H] $= -0.48$, and from the $(B-V)$ integrated colour, $E(B-V)=0.35$ (ZW84). Armandroff (1988) using $(V,\ I)$ CMDs found a metal-rich morphology compatible with ZW84's metallicity value, and derived $E(B-V)=0.30$.

The reddening in Table 3 is consistent with the $(V,\ I)$ CMDs, and the metallicity of all studies place the cluster in the MRBF. The cluster is not in a post-core collapse phase (TDK95).

4.20. NGC 6717

An early photographic CMD by Goranskii (1979) showed a blue HB at the detection limit and he derived $E(B-V) = 0.17$ and $[M/H] = -1.3$. By means of visible integrated spectroscopy, ZW84 found [Fe/H] $= -1.32$ and $E(B-V)=0.22$. Recently a deep V, $(B-V)$ CMD of NGC 6717 was presented by Brocato et al. (1996), where they adopted $E(B-V) = 0.22$ (from ZW84) and derived [Fe/H] $= -1.26$. Their CMD also shows a blue extended HB morphology for this post-core collapse cluster (TDK95), similarly to NGC 6522 (Barbuy et al. 1994). In the present sample, NGC 6717 is the only cluster in common with the large sample of globular clusters by Rutledge et al. (1997) who employed Ca II triplet of individual giants as metallicity indicator. They derived [Fe/H] $= -1.33$ in ZW84's metallicity scale and [Fe/H] $= -1.09$ in Carretta & Gratton's (1997) scale.

In addition to the total extraction (Table 1) we analyse a core extraction corresponding to $10''$ along the slit. The observed spectra are shown in the upper panel of Fig. 9. The core spectrum has a strong TiO band typical of bulge late-type stars, whereas in the total spectrum this feature is diluted, presumably by the cluster intrinsic stellar population, which is not metal-rich. The equivalent widths (Table 2) and metallicities derived for the total and core spectra (Table 3) are too high compared to the previous values, indicating important contamination. Contrary to HP 1, the contamination is stronger in the core. The reddening derived for the total spectrum (Table 3) is similar to that of ZW84.

A simple decontamination experiment can be carried out assuming that the contaminating bulge stars affect both spectra in different amounts. Our approach is to test different proportions for the core spectrum and subtract them from the total spectrum in order to cancel out the TiO band. The match was obtained for a proportion of 60% (flux fraction at ≈ 7500 Å), and the resulting decontaminated spectrum is shown in the lower panel of Fig. 9. By measuring Ws of the Ca II triplet (Table 2) we derive $[Z/Z_{\odot}] = -1.05$ (Table 3), which is now compatible with previous published values. NGC 6717 can be conclusively placed in the IMBF.

5. Clusters projected on the disk

Metal-rich globular clusters projected on the disk are particularly important because they may provide clues to a connection between the globular cluster system and the open cluster system. We note that recently another globular cluster projected on the disk, NGC 6749 ($l = 36.2°$, $b = -2.2°$), was studied by means of V, $(V-I)$ CMDs (Rosino et al. 1997; Kaisler et al. 1997). However, differently of the three cases discussed in the present paper, it is metal-poor and must be related to the halo family.

The spectra of the present sample of clusters projected on the disk are discussed in what follows, three of them are reinstated as probable globular clusters and two are open clusters.

5.1. BH 176

This object, located at Galactic coordinates $l = -31.6°$, $b = +4.3°$, has been studied by Ortolani et al. (1995b) in terms of $(V,\ I)$ CMDs, finding GB and HB morphologies of a metal-rich globular cluster. They derive $E(B-V) = 0.77$ and a metallicity $[M/H] \approx -0.4$.

The present spectroscopic reddening is somewhat lower but consistent with their value. The metallicity

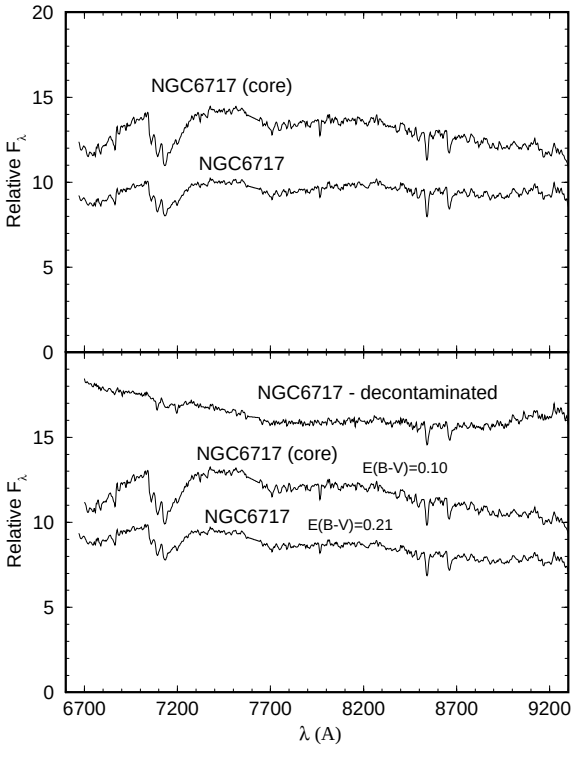

Fig. 9. Same as Fig. 8 for the core collapse case of NGC 6717. We also show the decontaminated spectrum according to Sect. 4.20

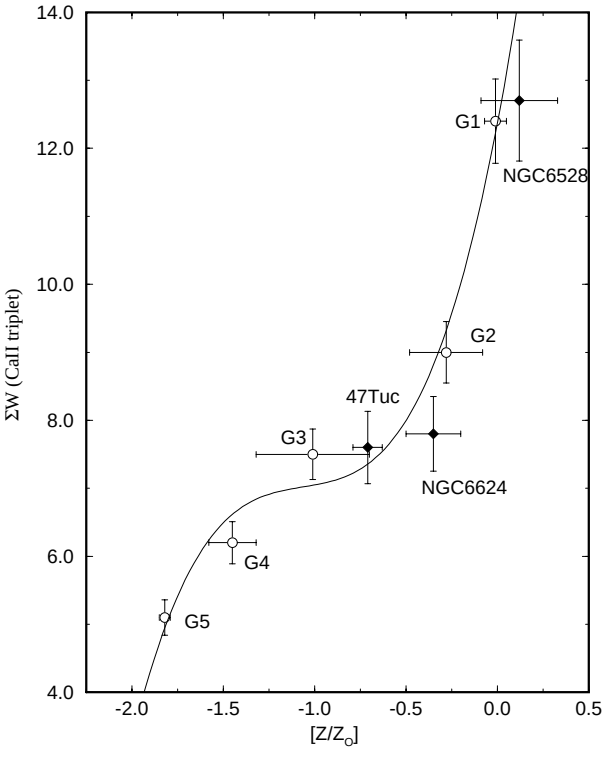

Fig. 10. Metallicity calibration for the sum of Ca II triplet equivalent widths

(Table 3) confirms that BH 176 is a metal-rich cluster. The cluster structure is similar to that of a loose globular cluster (see Fig. 1 in Ortolani et al. 1995b, and ESO/SERC Sky Survey field 224), but the number of stars would be unusually large for an open cluster.

5.2. Lyngå 7

This cluster at $l = -31.2°$, $b = -2.8°$ was suggested to be a globular cluster by Ortolani et al. (1993b) using $(V,\ I)$ CMDs. They found $E(B-V) = 0.72$ and $[M/H] \approx -0.4$, and detected GB and HB morphologies compatible to those of a metal-rich globular cluster, and also measured a value for the magnitude difference between the HB and the turnoff ($\Delta_{\rm HB}^{\rm TO} = 3.1$) comparable to those of young globular clusters like Ruprecht 106, Palomar 12, Arp 2, IC 4449 and Terzan 7 (Chaboyer et al. 1996). Lyngå 7 was reinstated as a likely globular cluster by Tavarez & Friel (1995) by means of spectroscopy of individual giants and from location, kinematics and metallicity arguments; they obtained $E(B-V) = 0.73$ and [Fe/H] $= -0.62$.

The present integrated spectroscopy (Table 3) confirms the previous reddening estimates and also indicates the cluster as metal-rich. The cluster structure is similar to that of a loose globular cluster (see Fig. 1 in Ortolani et al. 1993b, and ESO/SERC Sky Survey field 178), but likewise BH 176, it would be unusually populous for an open cluster.

5.3. Palomar 10

This cluster at $l = 52.4°$, $b = +2.7°$ was recently studied in V, $(V-I)$ CMDs by Kaisler et al. (1997), showing that the RGB and HB morphologies are those of a metal-rich globular cluster. They derived $E(B-V) = 1.66$ and estimated [Fe/H] $= -0.1$, and a concentration parameter $c = 0.58$, thus a loose cluster.

The present spectroscopic reddening and metallicity (Table 3) basically confirm their values.

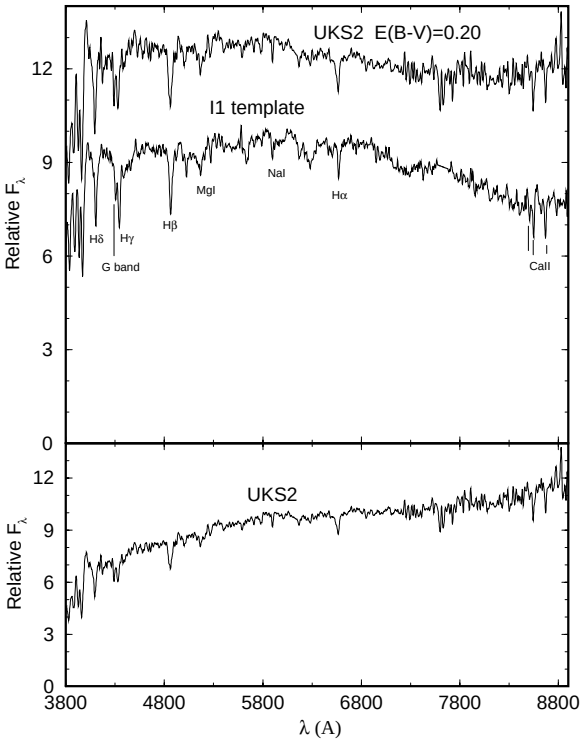

Fig. 11. Bottom panel: observed spectrum of UKS 2; top panel: reddening corrected spectrum of UKS 2 compared to the I 1 template ($t \approx 1$ Gyr). Main absorption features are labelled. Units as in Fig. 1

5.4. Open clusters

5.4.1. UKS 2

This cluster is located at $l = -84.0°$, $b = -3.0°$ and was included in the integrated infrared photometry by Malkan (1982) who obtained a reddening of $E(B-V) = 0.7$. ZW84 based on the same data estimated [Fe/H] $= -0.29$. Armandroff (1988) presented images of UKS 2 and suggested that it was an open cluster.

The integrated spectrum (Fig. 11) has strong Balmer lines typical of $t \approx 1$ Gyr clusters, as shown by the appropriate template match I 1, and the continuum distribution indicates that UKS 2 is affected by $E(B-V) = 0.20$ (Fig. 11, top panel). Since this is a rather loose cluster in a crowded disk field, contamination might be important, so it would be worth obtaining a CMD to check the derived reddening and age.

Since the integrated near-infrared light is essentially not affected by dilution effects of brighter turnoffs for young clusters, the Ca II triplet is a good metallicity indicator for intermediate age clusters, by adopting a globular cluster calibration (BA87). The metallicity obtained for this 1 Gyr cluster ($[Z/Z_\odot] = -0.15$) is consistent with that derived by ZW84.

5.4.2. ESO 93−SC08

A CMD of this object, at $l = -66.5°$, $b = -4.0°$, indicates that one is dealing with an old open cluster with age $\approx$ 4 Gyr (Bica et al. 1998).

In Fig. 12 we show the observed spectrum (bottom panel) and the reddening-corrected one ($E(B-V) = 0.35$) compared to the intermediate age template I 2 ($2 - 3$ Gyr) and the metal-rich globular cluster template G 2. From the continuum distribution, both lead to the same reddening value. Using the same arguments for an intermediate age cluster as discussed for UKS 2 above, we conclude that ESO 93−SC08 is metal-rich from the Ca II triplet ($[Z/Z_\odot] = -0.34$, Table 3). With respect to age, notice that the Balmer lines are particularly strong for this cluster, but not as much as in the 1 Gyr template (I 1). On the other hand, such Balmer enhancement is not observed in metal-rich globular clusters, such as the G 2 template. We conclude that the integrated spectrum of ESO 93−SC08 is consistent with that of an old open cluster.

6. Concluding remarks

In the present paper we studied a sample of reddened bulge globular clusters (and candidates) as well as some projected on the disk, by means of integrated near-infrared spectroscopy. The results, in conjunction with other available information from different observational techniques, especially recent CMDs, shed new light on their nature and properties. In particular we try to classify them into families.

Armandroff (1989) indicated a sample of 19 bona-fide metal-rich globular clusters, most of them towards the central regions of the Galaxy and not much reddened. To that list, the following 9 bulge clusters have been conclusively added: Terzan 2, NGC 6380, Tonantzintla 2, Palomar 6, Djorgovski 1, Terzan 5, Terzan 6, ESO 456−SC38 and Terzan 12 (with coordinates $\alpha_{1950} = 18^{\rm h}\ 09^{\rm m}\ 14.0^{\rm s}$ and $\delta_{1950} = -22°\ 45'\ 18''$). In addition, Palomar 8, already in Armandroff's list has its properties confirmed in the present study. Liller 1 and Terzan 1 are certainly members of the metal-rich bulge family, possibly among the most metal-rich ones; however, owing to crowding, contamination and reddening effects, deeper observations are necessary.

NGC 6256, HP 1 and NGC 6717 belong to an intermediate metallicity family in the bulge with $[Z/Z_\odot] = -1.0$ to -1.5 with prominent blue-extended HBs in post-core collapse clusters, similar to NGC 6522 (Barbuy et al. 1994)

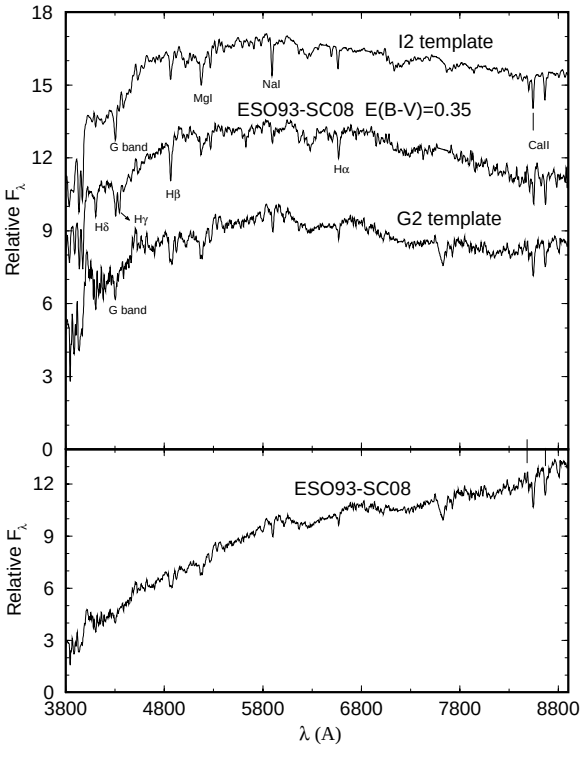

Fig. 12. Bottom panel: observed spectrum of ESO 93−SC08; top panel: reddening corrected spectrum of ESO 93−SC08 compared to the I 2 template ($t \approx 2 - 3$ Gyr), and the metal-rich globular cluster template G 2 ($[Z/Z_\odot] = -0.5$). Main absorption features are labelled. Units as in Fig. 1

and NGC 6540 (Bica et al. 1994). Terzan 9 probably belongs to this family, but deep CMDs are necessary to check. Terzan 10 is probably of intermediate metallicity but is not in a post-core collapse phase, and also requires deep CMDs for more conclusive results.

The integrated light of Terzan 4 is heavily contaminated by field stars; its nature appears to be that of a metal-poor globular cluster as recently unveiled by a deep CMD (Ortolani et al. 1997).

Although previous studies of the difficult globular cluster UKS 1 pointed to an intermediate metallicity, the present result indicates a metal-rich nature, unless the integrated light is contaminated by metal-rich field stars with reddening comparable to that of the cluster itself. The object requires deep CMDs to establish its properties.

From the present spectroscopic results, the object TBJ 3 = TJ 13 is reinstated as a globular cluster candidate and a deep CMD is required to establish its nature. It is expected that the dynamical evolution of globular clusters produces some post-core collapse fossils, after evaporation of their halos. TBJ 3 is the best candidate to be an example of such end products of cluster evolution.

For the clusters BH 176, Lyngå 7 and Palomar 10, which are projected on the disk, the present spectroscopic results show that they have a nearly-solar metallicity consistent with recent CMD studies which point them as metal-rich globular clusters. Such kind of object might be a link to the oldest solar-metallicity open clusters, like NGC 6791 ($l = +70.0°$, $b = +11.0°$) with age ≈ 8 Gyr (Demarque et al. 1992). Finally, ESO93SC−08 and UKS 2 are intermediate age open clusters, and the integrated spectroscopic results point to a subsolar metallicity.

We point out that quite often CMDs and integrated studies of reddened clusters in crowded fields show evidence of stellar population mixtures. The first interpretation in most cases would be contamination by field stars. Nevertheless, alternative interpretations like the possibility of mergers between globular clusters (Catelan 1997), and capture of field stars by globular clusters in dense bulge fields (Bica et al. 1997), might be explored by means of deep CMDs, velocities and abundance determinations of individual giants as membership criteria.

Acknowledgements. We thank the staff and personnel at CASLEO for hospitality and assistance during the observations. We acknowledge the Antorcha and VITAE foundations, the Argentinian institutions CONICOR and CONICET, and the Brazilian ones CNPq and FINEP for support.

References

Aguilar L.A., 1993, in Galaxy Evolution: the Milky Way Perspective, ASP Conf. Ser., Majewski S. (ed.). ASP, San Francisco, p. 155
Alcaino G., 1983, A&AS 53, 47
Alloin D., Bica E., 1989, A&A 217, 57
Armandroff T.E., 1988, AJ 96, 588
Armandroff T.E., 1989, AJ 97, 375
Armandroff T.E., Zinn R., 1988, AJ 96, 92 (AZ88)
Barbuy B., Castro S., Ortolani S., Bica E., 1992, A&A 259, 607
Barbuy B., Ortolani S., Bica E., 1994, A&A 285, 871
Barbuy B., Ortolani S., Bica E., 1997, A&AS 122, 483
Barbuy B., Ortolani S., Bica E., Renzini A., Guarnieri M.D., 1997, Fundamental Stellar Parameters: Confrontation Between Observation and Theory, Davis J., Booth A., Bedding T. (eds.). Kluwer Acad. Publ. (in press)
Bica E., 1988, A&A 195, 76
Bica E., 1994, A&A 285, 868
Bica E., Alloin, D., 1986a, A&A 162, 21
Bica E., Alloin, D., 1986b, A&AS 66, 171
Bica E., Alloin D., 1987, A&A 186, 49 (BA87)
Bica E., Barbuy B., Ortolani S., 1993, ApJ 382, L15
Bica E., Clariá J.J., Bonatto C., Piatti A.E., Ortolani S., Barbuy B., 1995, A&A 303, 747
Bica E., Dottori H., Rodrigues I.O.F., Ortolani S., Barbuy B., 1997, ApJ 482, L49
Bica E., Jablonka P., Santos J.F.C. Jr, Alloin D., Dottori H., 1992, A&A 260, 109

Bica E., Ortolani S., Barbuy B., 1994, A&A 283, 67
Bica E., Ortolani S., Barbuy B., 1996, A&AS 120, 153
Bica E., Ortolani S., Barbuy B., 1998 (in preparation)
Bica E., Pastoriza M.G., 1983, ApSS 91, 99
Brocato E., Buonanno R., Malakhova Y., Piersimoni A.M., 1996, A&A 311, 778
Bruzual G.A., Barbuy B., Ortolani S., Bica E., Cuisinier T., Lejeune T., Schiavon R.P., 1997, AJ 114, 1531
Buonanno R., Corsi C., Bellazzini N., Ferraro F.R., Fusi Pecci, F., 1997, AJ 113, 706
Carretta E., Gratton R.G., 1997, A&AS 121, 95
Catelan M., 1997, ApJ 478, L99
Chaboyer B., Demarque P., Sarajedini, A., 1996, ApJ 459, 558
Demarque P., Green E.M., Guenther D.B., 1992, AJ 103, 151
Djorgovski S., Meylan, G., 1993, in Structure and Dynamics of Globular Clusters, ASP Conf. Ser. 50, Meylan G., Djorgovski S. (eds.). ASP, San Francisco, p. 325
Djorgovski S., Thompson D.J., de Carvalho R.R., Mould J.R., 1990, AJ 100, 599
Frogel J.A., Kuchinski L.E., Tiede G.P., 1995, AJ 109, 1154
Geisler D., Piatti A.E., Clariá J.J., Minniti D., 1995, AJ 109, 605
Goranskii V.P., 1979, Soviet Astron. 23, 284
Guarnieri M.D., Ortolani S., Montegriffo P., Renzini A., Barbuy B., Bica E., Moneti A., 1998, A&A 331, 70
Gutiérrez-Moreno A., Moreno H., Cortés G., Wenderoth E., 1988, PASP 100, 973
Harris W.E., 1996, AJ 112, 1487
Jablonka P., Alloin D., Bica E., 1992, A&A 260, 97
Jablonka P., Bica E., Pelat D., Alloin D., 1996, A&A 307, 385
Jones J., Alloin D., Jones B., 1984, ApJ 283, 457
Kaisler D., Harris W.E., McLaughlin D.E., 1997, PASP 109, 920
Kuchinski L.E., Frogel J.A., Terndrup D.M., Persson S.E., 1995, AJ 109, 1131
Liu T., McLean I., Becklin E., 1994, in: Infrared Astronomy with Arrays, I. McLean (ed.). Kluwer Academic Publishers, p. 102
Malkan M.A., 1982, in Astrophysical parameters for globular clusters, Philip A.G.D., Hayes D.S. (eds.). Schenectady, Davis (M82) p. 533
Minniti D., 1995, A&A 303, 468
Minniti D., Olszewski E.W., Rieke M., 1995, AJ 110, 1686
Minniti D., Peterson R.C., Geisler D., Clariá J.J., 1996, ApJ 470, 953
Olszewski E.W., Schommer R.A., Suntzeff N.B., Harris H.C., 1991, AJ 101, 515
Origlia L., Ferraro F.R., Fusi Pecci F., Oliva E., 1997, A&A 321, 859
Ortolani S., Barbuy B., Bica E., 1991, A&A 249, L31
Ortolani S., Barbuy B., Bica E., 1996, A&A 308, 733
Ortolani S., Barbuy B., Bica E., 1997, A&A 319, 850
Ortolani S., Barbuy B., Bica E., 1998 (in preparation)
Ortolani S., Bica E., Barbuy B., 1993a, A&A 267, 66
Ortolani S., Bica E., Barbuy B., 1993b, A&A 273, 415
Ortolani S., Bica E., Barbuy B., 1995a, A&A 296, 680
Ortolani S., Bica E., Barbuy B., 1995b, A&A 300, 726
Ortolani S., Bica E., Barbuy B., 1996, A&A 306, 134
Ortolani S., Bica E., Barbuy B., 1997a, A&A 326, 614
Ortolani S., Bica E., Barbuy B., 1997b, MNRAS 284, 692
Ortolani S., Bica E., Barbuy B., 1997c A&AS 126, 319
Ortolani S., Bica E., Barbuy B., 1998, A&AS 127, 471
Ortolani S., Renzini A., Gilmozzi R., Marconi G., Barbuy B., Bica E., Rich R.M., 1995, Nat 377, 701
Peterson C.J., 1986, PASP 98, 1258
Piatti A.E., Bica E., Clariá J.J., 1998, A&AS 127, 423
Rosino L., Ortolani S., Barbuy B., Bica E., 1997, MNRAS 289, 745
Rutledge G.A., Hesser J.E., Stetson P.B., 1997, PASP 109, 907
Sanner F., Snell R., Vanden Bout P., 1978, ApJ 226, 460
Santos J.F.C. J., Bica E., Dottori H., Ortolani S., Barbuy B., 1995, A&A 303, 753
Seaton M.J., 1979, MNRAS 187, 73p
Stone R.P.S., Baldwin J.A., 1983, MNRAS 204, 347
Tavarez M., Friel E., 1995, AJ 110, 223
Terzan A., 1971, A&A 12, 477
Terzan A., Bernard A., 1978, ESO Messenger 15, 14
Terzan A., Ju K.H., 1980, ESO Messenger 20, 6
Trager S.C., Djorgovski S., King I.R., 1993, in Structure and Dynamics of Globular Clusters, ASP Conf. Ser. 50, Meylan G., Djorgovski S. (eds.). ASP, San Francisco, 347 (TDK93)
Trager S.C., King I.R., Djorgovski S., 1995, AJ 109, 218
van den Bergh S., 1996, PASP 108, 986
Webbink R.F., 1985, in Dynamics of Star Clusters, IAU Symp. 113, Goodman J., Hut P. (eds.). Dordrecht, Reidel, p. 541
Zinn R., 1980, ApJS 42, 19
Zinn R., 1985, ApJ 293, 424 (Z85)
Zinn R., West M.J., 1984, ApJS 55, 45 (ZW84)